14,09,03

Amplitude-dependent internal friction and modulus of elasticity in single crystal of Ga_2O_3-Al_2O_3 solid solution

© D.A. Kalganov[1,2], D.A. Bauman[1], D.Yu. Panov[1], V.A. Spiridonov[1], A.Yu. Ivanov[1,2], A.E. Romanov[1]

[1] ITMO University,
St. Petersburg, Russia
[2] Ioffe Institute,
St. Petersburg, Russia

E-mail: d.a.kalganov@mail.ioffe.ru

Received October 2, 2025
Revised October 2, 2025
Accepted October 4, 2025

The oscillatory deformation in single crystals of the Ga_2O_3-Al_2O_3 solid solution was investigated using the composite piezoelectric oscillator method. The amplitude and temperature dependencies of the damping decrement and the modulus of elasticity were obtained. The presence of amplitude-dependent internal friction, associated with the microplasticity effect in the material under study, was demonstrated. Thermoactivated relaxation effects of elastic oscillations were observed in the studied material at low temperatures $T_1 \approx 134$ K and $T_2 \approx 182$ K. It was established that aluminum ions in the studied solid solutions form diffusion fields for mobile dislocations and determine the features of the amplitude-dependent internal friction.

Keywords: internal friction, modulus of elasticity, microplasticity, composite piezoelectric oscillator, gallium oxide, defects.

DOI: 10.61011/PSS.2025.10.62648.269-25

1. Introduction

Semiconductor materials based on beta phase crystals of gallium oxide (β-Ga_2O_3) gain considerable attention from scientific groups worldwide [1–4] due to the prospects of their use in power electronics, UV detectors and other optoelectronics [5,6]. The advantages of the beta phase of gallium oxide include a large band gap of 4.8 eV, high thermal stability and radiation resistance. The ability to grow β-Ga_2O_3 single crystals from the melt has stimulated research on the fabrication of substrates and bulk components for semiconductor devices in this area [1,7,8]. The functional properties of Ga_2O_3 are largely determined by its defect structure, in particular, vacancies of various types, impurity centers that occur during growth and defects introduced during processing [1,9]. One of the significant areas of work in the growth of bulk crystals of gallium oxide is the creation of solid solutions of Ga_2O_3-Al_2O_3 [10]. Aluminum ions can be distributed in such crystals along octahedral and tetrahedral positions of the sub-lattice Ga^{+3} while maintaining a monocrystalline low-defect structure of β-Ga_2O_3 in a large concentration range (to mol. 40 % [11]). At the same time, the resulting solid solution is characterized by higher values of the band gap [10,11] and can be used as a platform for design of new devices.

The study of mechanism of energy dissipation in the process of oscillatory deformation — internal friction (IF, δ), as well as effective modulus of elasticity (EM, E) in the single crystals of β-Ga_2O_3 is extremely relevant in terms of both, fundamental science, and practical usage. The ability of materials to dissipate the energy of mechanical vibrations during cyclic deformation characterizes the microstructure of a material and, in case of single crystals, is closely related to the presence of various defects in them. The analysis of the nonlinear amplitude-dependent part of internal friction (ADIF) and the modulus of elastic modulus softening (EMS) in the region of high ($\sim 10^5$ Hz) frequencies makes it possible to determine the presence of mobile defects and analyze the effects of elastic stress relaxation due to their interaction [3,9].

The composite piezoelectric oscillator (CPO) method is an experimental method for studying the mechanical properties and defect structure of crystalline materials, which makes it possible to register the values of IF and EMS in the high frequency band [12]. The essential requirements of CPO for the geometry of samples and the uneven distribution of oscillatory stresses in them require a special approach in the process of preparing single-crystal samples to characterize their defective structure. The presence of surface disturbances in the crystal structure can have an impact on the measured CPO values. Thus, in the case of materials with a strong interatomic interaction, e.g., Al_2O_3 ceramics [13], it was shown that the defects started to move because of internal stresses in the material, which were concentrated in areas of microdefects, for example, in the tops of microcracks. This is confirmed by observations in the work of [13] of microplastic deformation under stresses two orders of magnitude lower than the macroscopic yield point, as well as a symmetrical hysteresis loop [14], characteristic of the frictional mechanism of energy dissipation. Previously, the CPO method was used

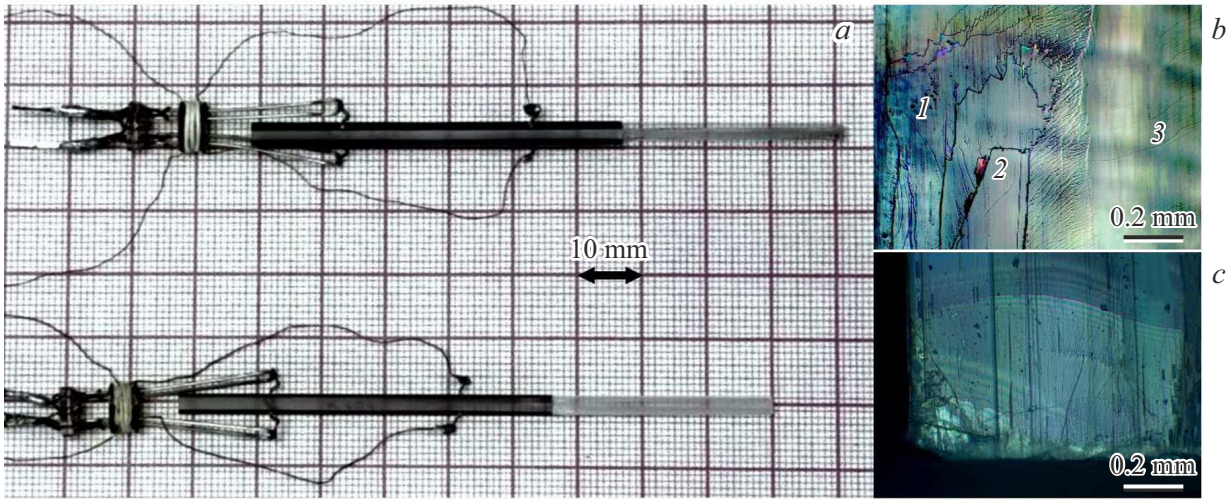

Figure 1. The appearance of samples fixed on a quartz transducer (*a*), images of parts of the sample obtained by optical microscopy in polarized light (*b*) and (*c*). The digits *1, 2, 3* denote, respectively, inclusions (gas inclusions), cleavages, and a monocrystalline region with traces of growth bands.

to describe the elastic properties and microplasticity of ionic crystals, including the ultra-wide-band semiconductor gallium nitride (see [15]). The anisotropy of EMS and IF in GaN was explained both by dependence on the crystal orientation and by anisotropy in the defect distribution due to the material preparation method.

In the case of solid solutions, the strain amplitude dependences obtained by the CPO method make it possible to separate the mechanisms of interaction of dislocations with impurity atoms localized in the dislocations slip planes, which are overcome in a thermally activated mode, and with impurity atoms that affect dislocations due to elastic interaction, which are overcome in athermic conditions [16]. For solid solutions based on ionic crystals Ga_2O_3-Al_2O_3, when interpreting the data and separating the contributions of internal friction mechanisms, it becomes necessary to take into account complex defect formation involving various types of oxygen (V_O) and gallium (V_{Ga}) vacancies, substitution atoms (Al_{Ga}), their complexes, as well as the structural state of the samples due to the method of their preparation and treatment.

This study is devoted to the examination of microplastic deformation in single crystals of the Ga_2O_3-Al_2O_3 solid solution through the measurements of amplitude-dependent internal friction and modulus of elasticity using the CPO method at a frequency of about 100 kHz. The analysis of the data obtained by CPO method is aimed at finding the relationship between the defective structure and the structure-dependent characteristics of the material, determining the total contribution of the defective structure of the material to elastic vibrations damping, as well as describing the effect of dislocations interaction with the fields of barrier and long-range defects on the internal friction.

2. Experimental procedure

We studied samples as rectangular cross-section bars (Figure 1, *a*) with characteristic dimensions $2\times3\times32$ mm cut from bulk crystals of a solid solution Ga_2O_3-Al_2O_3, obtained by growth from the melt [10]. The cut samples were examined using optical microscopy image analysis in polarized reflected light (microscope MET-5T, Altami). Bragg–Brentano diagram was used for X-ray measurements using Cu-K_α emission and standard slit configuration diffractometer DRON-8 (Burevestnik). To study the oscillatory deformation, the method of a composite piezoelectric oscillator based on quartz transducers [12] was used at an excitation frequency of about 100 kHz and a relative strain amplitude from 10^{-7} to 10^{-4}. The direction of propagation of elastic vibrations (ultrasound) coincided with the long side of the bar and with the crystallographic direction [010] in the beta-phase lattice of Ga_2O_3-Al_2O_3, which was the crystal's growth direction and along which the samples were cut. Photographs of the studied samples mounted on a quartz transducer, similar to [9], as well as images obtained using optical microscopy, are shown in Figure 1.

The values of the damping decrement δ, corresponding to IF in the material, the resonant frequency f of vibrations and the relative strain amplitude ε were measured using CPO method. The amplitude dependences were studied with a monotonic increase (forward run) of ε from the initial value ε_0, corresponding to the stable excitation of CPO resonant vibrations at small strain amplitudes $\varepsilon_{max} \sim 10^{-7}$, to the maximum $\varepsilon_{max} \sim 10^{-4}$ and its decrease (reverse run) to values corresponding to the initial conditions. To study the temperature dependences, cooling and heating modes with a rate of no more than 2 K/min were used with the help of a low-temperature tool similar to that described in [17].

The methodology for processing the data obtained by CPO, calculating the amplitude-dependent internal friction and modulus of elasticity, is described in more detail in papers [9,12,18]. The amplitude-dependent internal friction (δ_d), and elastic modulus softening $(\Delta E/E)_d$ were defined similar to these studies relative to the values (E_0, δ_0), measured at small $\varepsilon \sim 10^{-7}$ strain amplitudes.

$$\delta = \delta_0 + \delta_d \tag{1}$$

$$(\Delta E/E)_d = \frac{(E - E_0)}{E_0} \tag{2}$$

Also, based on the measured values the coefficient r of ADIF and EMS proportionality was additionally found:

$$\delta_d = r(\Delta E/E)_d \tag{3}$$

The magnitude of this coefficient was used to determine the type of dislocation interaction with the barriers to be overcome, and the spatial distribution of defects acting as these barriers was determined by the amplitude dependence $r(\varepsilon)$.

Previously obtained data on the study of pure crystals of β-Ga_2O_3 the CPO method is given in [3,9].

3. Experimental Results

3.1. Optical microscopy

Optical microscopy images of the studied samples made it possible to visualize areas containing various macroscopic defects, both related to the crystal growth method (Figure 1, *b*) and caused by the preparation (cleaving, cutting) of the samples (Figure 1, *c*). The largest area of the disturbed structure in the studied samples was located at the bars ends and did not exceed 0.8 mm from their edge. In the central part of the samples studied by the acoustic technique, which makes the greatest contribution to the measured characteristics, a system of parallel bands formed during crystal growth was observed (see for example, „striations“ [19]).

3.2. X-ray diffractometry

The X-ray diffraction data obtained for the studied crystal in the range of angles $2\theta = 10° - 120°$ and the diffraction reflection curve under the reflex conditions 4 0 0 are shown in Figure 2.

When studying the central area of the sample a series of diffraction reflections corresponding to plane (1 0 0) of beta-phase Ga_2O_3-Al_2O_3 was observed (Figure 2, *a*). The width of the diffraction reflection curve 4 0 0 at full width at half maximum (FWHM) for the studied crystal was 75″.

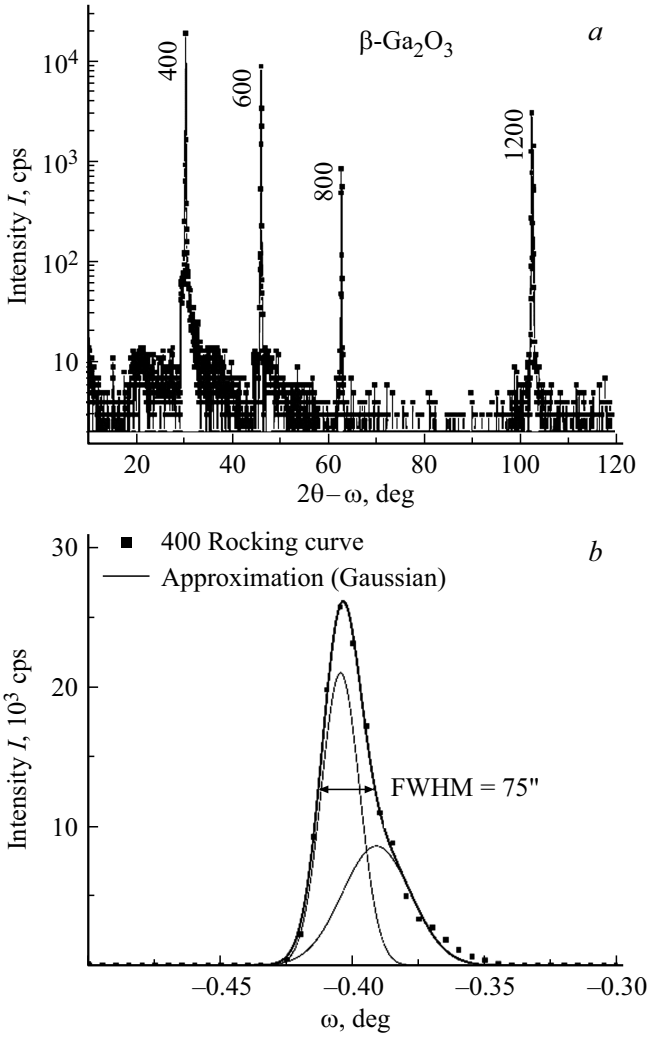

Figure 2. X-ray diffraction pattern (*a*) and rocking curve (*b*) in reflection conditions 4 0 0.

3.3. Studies by CPO method

For small strain amplitudes $\varepsilon \approx 10^{-7}$, the values of the modulus of elasticity $E_0 = 292$ GPa, and the damping decrement of elastic vibrations $\delta_0 = 8 \cdot 10^{-7}$ were found. The amplitudes dependencies of the IF decrement $\delta = \delta(\varepsilon)$ were obtained at gradual increase of $\varepsilon_{\max}$ to 10^{-4}. At the same time, hysteresis was observed with an increase in the initial measured values of the decrement δ_0 and maintaining ADIF for forward and reverse strokes (cycles 0-2 in Figure 3, *a*). When $\varepsilon_{\max} \approx 10^{-5}$ was reached, there was a change in the dependence (an inflection in ADIF curves) with a sharp increase in the values of δ_0 during the reverse course (cycles 2-5 in Figure 3, *a*). Further measurements showed a decrease in the initial value of the decrement (cycles 5-10, in Figure 3, *a*).

The values of the modulus E declined with the rise of strain amplitude, which corresponds to a positive value of EMS. Also, the values of E were less than the corresponding values during the reverse run — negative hysteresis caused

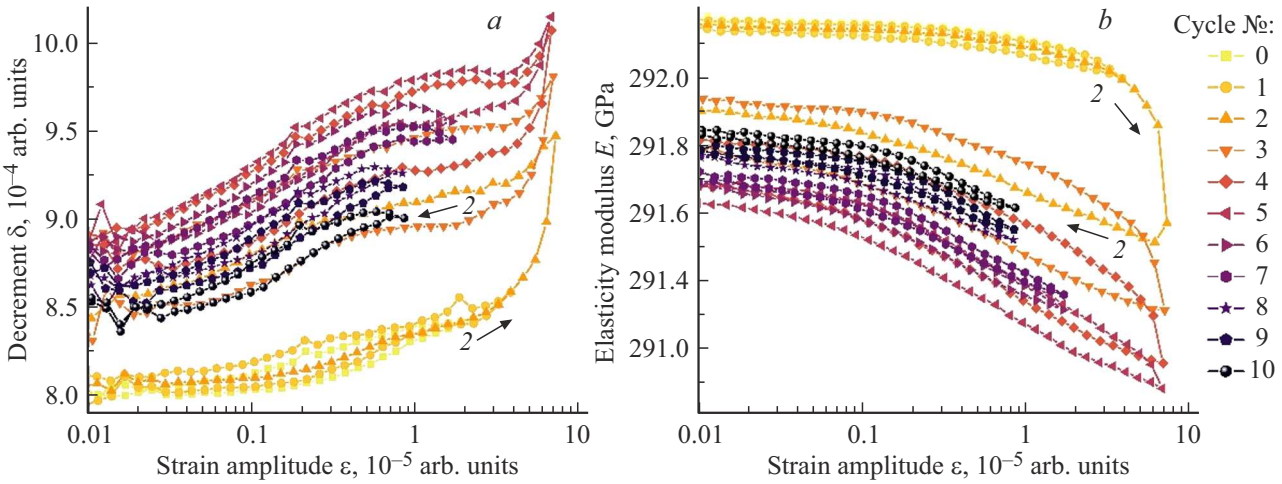

Figure 3. Internal friction decrement δ (a) and effective modulus of elasticity E (b) versus oscillatory strain amplitude. The numbers indicate the sequence of loading cycles, the arrow shows an increase in the amplitude of strain (forward run) and its decrease (reverse run) for cycle 2.

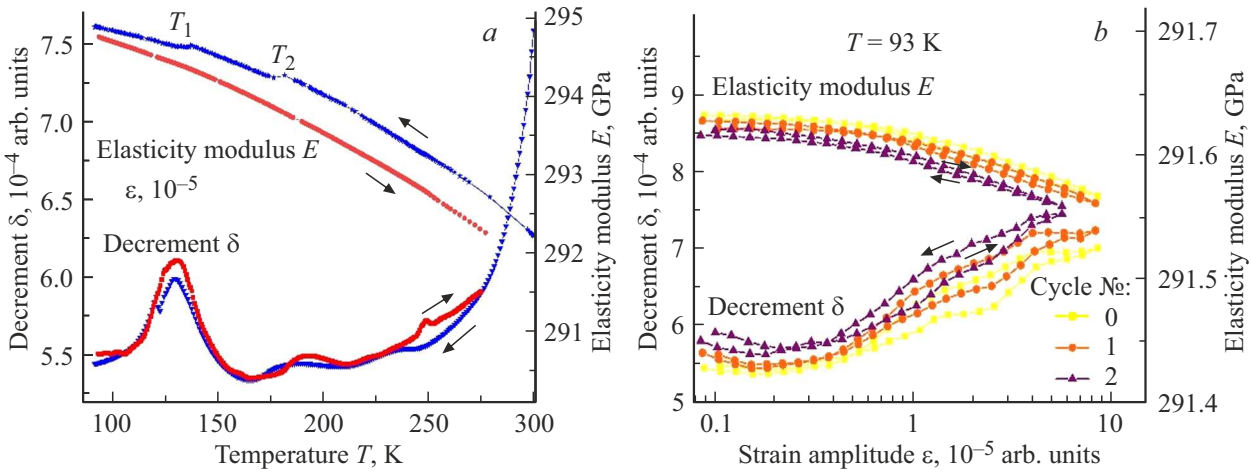

Figure 4. Internal friction decrement δ and effective elasticity modulus E versus temperature (a) and versus strain amplitude of oscillatory deformation at a temperature of 93 K (b). The arrows indicate the directions of temperature variation and the strain amplitude, the colors — measurement cycles.

by a decrease in (vibrational) elasticity (Figure 3, b). For threshold values $\varepsilon_{max} \approx 10^{-5}$, the behavior opposite to δ_0 is observed — a change in the amplitude dependence $E(\varepsilon)$ and a sharp decrease in absolute values while maintaining the magnitude of the relative change.

The data of temperature dependencies of modulus E and decrement δ during cooling and heating of crystal $Ga_2O_3-Al_2O_3$ for the strain amplitude $\varepsilon_{max} = 10^{-6}$ are given in Figure 4, a. This strain rate in the samples, when obtaining temperature dependences, was selected based on the data in Figure 3, as corresponding to the beginning of ADIF. The modulus of elasticity increases almost monotonously with decreasing temperature, which reflects the standard thermal behavior of the Young's modulus in crystalline bodies. The relative change in the modulus $\Delta E \approx 0.8\,\%$ is maintained when the sample is cooled to 93 K and heated to 273 K. The dependence $E(T)$ has inflections in points $T_1 \approx 134$ K and $T_2 \approx 182$ K. The internal friction in the studied samples decreases with the temperature decline (Figure 4, a — decrement δ). The change $\delta(T)$ has a non-monotonic nature with local maxima at temperatures T_1 and T_2. For the minimum cooling temperature $T = 93$ K, a sequence of measurements of E and δ with a change in the maximum strain amplitude was obtained, similar to Figure 3. The IF decrement at low temperature went up with the growing amplitude, similar to the high-temperature dependences, but it practically did not change between measurement cycles (Figure 4, b).

The proportionality coefficient r of ADIF δ_d and EMS $(\Delta E/E)_d$ for room and low-temperature measurements did not exceed the value 2, but in both cases showed a pronounced dependence on the strain amplitude (Figure 5).

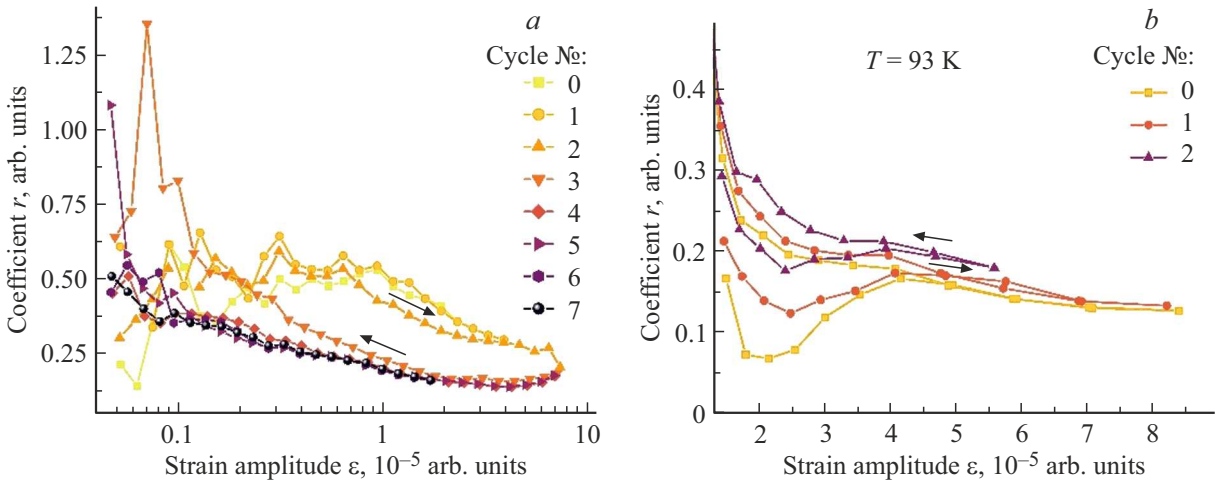

Figure 5. The proportionality coefficient r of the amplitude-dependent friction δ_d and elastic modulus softening $(\Delta E/E)_d$ for the room (a) and low-temperature (b) changes. The numbers indicate the sequence of loading cycles, the arrow shows an increase in the strain amplitude (forward run) and its decrease (reverse run).

The effect of a change in IF δ_0 upon reaching the maximum strain amplitude $\varepsilon_{\max} \approx 10^{-5}$ changed the dependence $r(\varepsilon)$ and decreased its absolute value at room temperatures (Figure 5, a), while at low temperatures, the dependence $r(\varepsilon)$ corresponded to the state of the already deformed sample (Figure 5, b).

4. Discussion of results

Heterogeneities in the form of growth bands were observed in the entire volume of the studied samples (region *3* in Figure 1, b), which could be formed due to heterogeneity in the distribution of vacancies (V_O,V_{Ga}) and substitution atoms (Al_{Ga}), or by changing the crystal growth conditions. It is well known that the appropriate defects (striations), as well as associated dislocation structures and microcracks are formed in the crystals of β-Ga_2O_3 grown along the direction [0 1 0] by various methods [20,21]. The influence of macroscopic defects of a different kind (regions *1, 2* in Figure 1, b) and crystal disturbances as a result of cutting was excluded in this study due to sampling and the peculiarities of the applied technique — distribution of vibrational stresses in the sample [22].

According to X-ray diffraction (Figure 2) the pseudo-cubic parameter $a^{pc}_{Ga_2O_3} = 3.74$ Å was found. Using the Vegard linear approximation and the corresponding parameter for the aluminum oxide lattice $a^{pc}_{Al_2O_3} = 3.59$ Å [23], the molar fraction of aluminum in the studied solid solution was determined to be ~ 3.5 %. The broadening of the diffraction curve (Figure 2, b) in the region of large angles may indicate a change in the parameter in a small range of values for individual regions of the crystal. Taking into account the X-ray analysis data, at low values of the aluminum content in the lattice (up to at.10 %), Al_{Ga} aluminum atoms replace gallium atoms only in octahedral positions [10]. The presence of aluminum ions in these positions produce diffuse [16] elastic fields that affect dislocations moving in the slip systems. However, even a small degree of substitution of Al_{Ga} has a significant effect on the defective structure of the sample, in particular on the presence of various types of vacancies, as well as on the appearance of impurity bands (growth bands) in the sample.

The obtained data for the modulus of elasticity $E \approx 294$ GPa and the applied technique with maximum strain amplitudes $\varepsilon_{\max} \approx 10^{-5}$ allow us to estimate the stresses $\sigma_{\max} < 300$ MPa occurring in the center of the sample. However, the presence of high internal stresses and microcracks indicates the possible mobility of dislocations and point defects in the crystal under study, despite the high critical shear stresses in it (see, for example, [4], the shear modulus in various slip system for the direction of [0 1 0] not less than 3.9 GPa). The minimum value of IF $\delta_0 = 8 \cdot 10^{-4}$ is determined by micro-processes unrelated to microplasticity: bowing of dislocation segments and thermoelastic effects. The microplastic deformation in the studied samples, corresponding to ADIF and the change in EM in Figure 3, similarly to [13] is determined by their defective state at various levels — the presence of microcracks and dislocation structures (walls) as a source of mobile dislocations, as well as the interaction of mobile dislocations in these areas with other defects.

The presence of local maxima $\delta(T)$ corresponding to a change in elasticity $E(T)$ at temperatures T_1 and T_2 (Figure 4, a) demonstrates thermally activated relaxation processes of mechanical stresses. Light impurities (C^+, Si, etc.), or complexes of oxygen vacancies with donor impurities may be considered as appropriate defects. Aluminum ions, due to the low degree of substitution, are a source of long-range forces and cause IF corresponding to the decreasing part of the dependence $r(\varepsilon)$ for the sample after a high degree of deformation at room temperature

(cycles 4-7 in Figure 5, *a*) and constant dependence at low temperatures (Figure 5, *b*).

5. Conclusions

For single crystals of Ga_2O_3-Al_2O_3 solid solution, the values of the elasticity modulus $E_0 = 292$ GPa and decrement of elastic vibrations $\delta_0 = 8 \cdot 10^{-4}$ decay were measured at small strain amplitudes (purely elastic deformation), corresponding to the fundamental elastic and relaxation characteristics of the material. Compared to β-Ga_2O_3 crystals fabricated and studied under the same conditions, an increase in the elastic modulus ($E_0^{Ga_2O_3} = 260$ GPa [9]) was observed. The studied crystals show the presence of amplitude-dependent internal friction associated with the effect of microplasticity and caused by thermally activated interactions of mobile dislocations with defects. The relaxation effects associated with the presence of vacancies and previously detected in crystals of β-Ga_2O_3 were not observed in the studied crystals. Aluminum ions in the studied solid solution of Ga_2O_3-Al_2O_3 generate the diffuse fields, which is proved by the specifics of dislocation internal friction and confirmed by the amplitude dependence of the coefficient $r(\delta)$, obtained by low-temperature measurements.

Funding

This study was carried out with financial support provided by the Russian Science Foundation (grant No. 24-12-00229, https://rscf.ru/project/24-12-00229/

Conflict of interest

The authors declare that they have no conflict of interest.

References

[1] R.M. Lavelle, W.J. Everson, D.J. Erdely, L.A.M. Lyle, S.W. Pistner, S.R. Hallacher, J.M. Redwing, D.W. Snyder. Mater. Sci. Semicond. Process. **190**, 109341 (2025).
[2] Y. Yan, C. Li, N. Xia, T. Deng, H. Zhang, D. Yang. Phys. Rev. Appl. **21**, *6*, 064036 (2024).
[3] V.V. Kaminsky, D.A. Kalganov, D.Yu. Panov, V.A. Spiridonov, A.Yu. Ivanov, M.V. Rozayeva, D.A. Bauman, A.E. Romanov. Kond.sredy mezhfaznoy granitsi **25**, *4*, 548 (2023).
[4] D. Wu, Y. Yan, X. Sun, X. Gao, D. Liu, Y. Liu, Z. Jin, N. Xia, H. Zhang, D. Yang. J. Alloy. Compd. **1018**, 179092 (2025).
[5] D.J. Valdes, L. Rendon, J. Winkelbauer, P. Koehler, S.C. Vogel, K.-X. Sun. APL Mater. **13**, 4 (2025).
[6] K.D. Shivani, A. Ghosh, M. Kumar. Mater. Today Commun. **33**, 104244 (2022).
[7] D.A. Bauman, D.Iu. Panov, V.A. Spiridonov, A.V. Kremleva, A.V. Asach, E.V. Tambulatova, A.V. Sakharov, A.E. Romanov. J. Vac. Sci. Technol. A **41**, 053203 (2023).
[8] Z. Galazka. J. Appl. Phys. **131**, 3 (2022).
[9] V.V. Kaminskii, D.Yu. Panov, V.A. Spiridonov, D.A. Bauman, D.A. Kalganov, M.P. Scheglov, A.E. Romanov. Mater. Phys. Mech. **52**, *5*, 48 (2024).
[10] D.A. Zakgeim, D.A. Bauman, D.I. Panov, V.A. Spiridonov, A.V. Kremleva, A.S. Smirnov, M.A. Odnoblyudov, A.E. Romanov, V.E. Bougrov. Appl. Phys. Express **15**, 025501 (2022).
[11] Z. Galazka, A. Fiedler, A. Popp, P. Seyidov, S.B. Anooz, R. Blukis, J. Rehm, K. Tetzner, M. Pietsch, A. Dittmar, S. Ganschow, A. Akhtar, T. Remmele, M. Albrecht, T. Schulz, T.-S. Chou, A. Kwasniewski, M. Suendermann, T. Schroeder, M. Bickermann. Adv. Mater. Interfaces **12**, *2*, 2400122 (2025).
[12] S. Kustov, S. Golyandin, A. Ichino, G. Gremaud. Mater. Sci. Eng. A **442**, *1-2*, 532 (2006).
[13] Y. Nishino, H. Ogawa, S. Asano. Philos. Mag. Lett. **66**, *6*, 313 (1992).
[14] Y. Nishino, T. Murayama, S. Asano. Philos. Mag. A **65**, *5*, 1187 (1992).
[15] L.I. Guzilova, B.K. Kardashev, A.I. Pechnikov, V.I. Nikolaev. ZhTF **90**, *1*, 138 (2020). (in Russian).
[16] G. Gremaud, S. Kustov. Phys. Rev. B **60**, *13*, 9353 (1999).
[17] D.A. Kalganov, V.V. Kaminskii, N.M. Yurchenko, N.M. Silnikov, I.V. Guk, A.I. Mikhailin, A.V. Podshivalov, A.E. Romanov. Rev. Adv. Mater. Technol. **4**, *1*, 14 (2022).
[18] A.B. Lebedev. FTT **41**, *7*, 1214 (1999). (in Russian).
[19] W.E. Langlois. Annu. Rev. Fluid Mech. **17**, 191 (1985).
[20] Y. Wang, X. Li, Y. Wu, D. Mu, H. Huang. Int. J. Mech. Sci. **204**, 106562 (2021).
[21] D. Dhanabalan, S.M. Babu. Mater. Sci. Semicond. Process. **194**, 109600 (2025).
[22] A.S. Nowick. Phys. Rev. **80**, *2*, 249 (1950).
[23] H. Peelaers, J.B. Varley, J.S. Speck, C.G. Van de Walle. Appl. Phys. Lett. **112**, 242101 (2018).

Translated by T.Zorina